

Study on Rotational Relaxation in a Steady Hydrogen Plasma Jet Using Emission Spectroscopy

Yoshiki Takama* and Kojiro Suzuki†
University of Tokyo, Kashiwa, Chiba 277-8561, Japan

DOI: 10.2514/1.46201

Rotational relaxation collision number of molecular hydrogen was experimentally determined using a steady plasma jet and emission spectroscopy. The plasma jet reached translational-rotational nonequilibrium by the strong free expansion at an orifice installed at the entrance of the test section, and translational-rotational relaxation occurred downstream of the orifice. Because the plasma jet was emissive, the translational and rotational temperatures could be directly measured using emission spectroscopy. The rotational relaxation collision number of molecular hydrogen calculated based on these measured temperatures was 70–150 for the temperature range of 500–700 K. These results support two of the latest theoretical studies, thus demonstrating the validity of this methodology to determine the relaxation collision number.

Nomenclature

$C_{v,vib}$	= specific heat of vibrational mode of molecular hydrogen, $\text{J kg}^{-1} \text{K}^{-1}$
d	= molecular diameter of hydrogen, m
d_{ref}	= reference molecular diameter of hydrogen in variable hard sphere model, m
k	= Boltzmann constant, $1.381 \times 10^{-23} \text{ J/K}$
m	= molecular weight of hydrogen, 2.0 g/mol
n	= number density, m^{-3}
p	= static pressure, Pa
p_0	= total pressure, Pa
R	= gas constant of molecular hydrogen, $4125 \text{ J kg}^{-1} \text{K}^{-1}$
T_e	= electron temperature, K
T_r	= rotational temperature, K
T_{ref}	= reference translational temperature in variable hard sphere model, K
T_s	= equilibrium temperature between translational and rotational modes, K
T_t	= translational temperature, K
T_v	= vibrational temperature, K
u	= flow velocity, m/s
v_{th}	= thermal velocity, m/s
x	= axial coordinate, mm
Z_r	= rotational relaxation collision number
γ	= specific heat ratio
λ	= mean free path, m
θ_v	= characteristic temperature of vibrational excitation of molecular hydrogen, 6159 K
τ_c	= mean collision time between molecular hydrogen, s
ω	= viscosity index in variable hard sphere model
τ_r	= translational-rotational relaxation time, s

I. Introduction

THE rotational relaxation collision number is the number of collisions required to relax the rotational energy to translational

energy. The Z_r of hydrogen [1–8] is much larger than that of either nitrogen or oxygen [5,9–11], indicating much slower translational-rotational relaxation in hydrogen. Therefore, for hydrogen, the T_r might not be considered equal to T_t though equilibrium between these two temperatures is often applicable in nitrogen and oxygen. In numerical simulations of hydrogen nonequilibrium flow [12,13], T_r is treated as another variable, which has a different value from T_t . In such simulations, the rotational relaxation is calculated based on Z_r or on τ_r . Although Z_r of molecular hydrogen has been extensively investigated both theoretically and experimentally [1–8], large variation in the obtained Z_r is evident, as shown in Fig. 1. More accurate determination of Z_r of molecular hydrogen is necessary.

One theoretical approach for the determination of Z_r of molecular hydrogen is state-to-state simulations using the rovibrational master equations [3,4]. This is the most rigorous approach. However, the state-to-state rate coefficients are not completely available for every possible transition because molecules have a large number of levels in general. Even though they are available or calculated, uncertainty in them can be large. Another theoretical approach is the QCT (quasi-classical trajectory) method [2], where the collisional processes are calculated based on classical theory. However, the results of the QCT method depend on the intermolecular potential model. In contrast to ongoing theoretical research, experimental research on the Z_r of molecular hydrogen was mainly done only in the 1960s–1970s [5–7], and as far as the authors know, no recent experimental attempts have been reported, despite the wide scatter in the data for Z_r of molecular hydrogen shown in Fig. 1. Increasing the experimental data is needed to assess theoretical results and to improve the relaxation models.

Representative experimental methods to study the relaxation processes in gases include using a shock wave and a freejet. Boitnott and Warder [6] used a shock tube to study Z_r of molecular hydrogen because a shock tube reliably generates strong shock waves, thus allowing observation of the relaxation processes behind the shock wave. In their study, Boitnott and Warder measured the density profiles behind the shock wave by using an electron beam transmitted across a shock tube normal to the axis of the propagating shock wave. Although attenuation of the electron beam is related to the gas number density, deduction of Z_r from the results is not an easy task, and considerable uncertainty can be introduced [14]. Based on the speculations described in [7], Boitnott and Warder fitted the experimental shock wave thickness with the calculated one. However, this depends on the position of the downstream edge of the shock wave, which is difficult to locate. Moreover, not only for the experiments by Boitnott and Warder, generally, high time resolution is required for measurements that use a shock tube, and the shock front becomes curved due to boundary-layer growth along the wall [3]. Regarding a freejet method, Gallagher and Fenn [7] produced a nonequilibrium jet by strong free expansion, and investigated the

Received 30 June 2009; revision received 12 March 2010; accepted for publication 17 March 2010. Copyright © 2010 by the American Institute of Aeronautics and Astronautics, Inc. All rights reserved. Copies of this paper may be made for personal or internal use, on condition that the copier pay the \$10.00 per-copy fee to the Copyright Clearance Center, Inc., 222 Rosewood Drive, Danvers, MA 01923; include the code 0887-8722/10 and \$10.00 in correspondence with the CCC.

*Graduate Student, Japan Society for the Promotion of Science Research Fellow, Department of Advanced Energy, 5-1-5 Kashiwanoha. Currently, Researcher, Japan Aerospace Exploration Agency; takama.yoshiki@jaxa.jp. Member AIAA.

†Professor, Department of Advanced Energy, 5-1-5 Kashiwanoha; kjsuzuki@k.u-tokyo.ac.jp. Member AIAA.

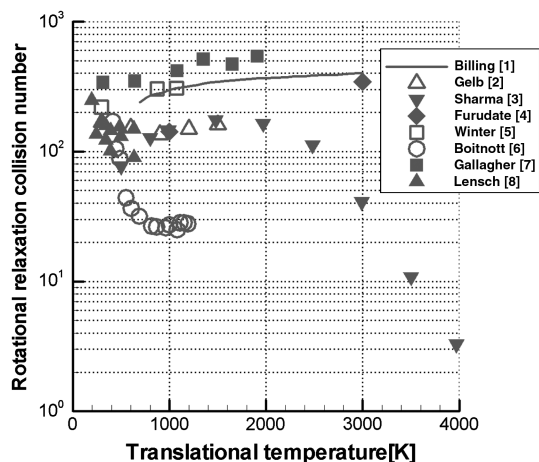


Fig. 1 Rotational relaxation collision number of molecular hydrogen reported in the literature.

relaxation processes between translational and rotational modes of various molecules. They extracted a molecular beam from the freejet by using a chopper, and then measured the velocity of the beam by using the time-of-flight technique [15]. The measured velocity distribution of the beam yielded T_t and the mean flow velocity of the jet, and T_r was calculated based on the energy balance. Based on the measurement data, Gallagher and Fenn then directly determined Z_r as a function of T_t .

In the present study, a method to determine Z_r by using a steady nonequilibrium plasma jet and emission spectroscopy was proposed. A plasma jet was used, because its emission enables temperature measurements by emission spectroscopy. The translational-rotational relaxation process of molecular hydrogen was investigated by directly measuring T_t and T_r along the steady jet by using emission spectroscopy. Because our plasma jet was steady, our method has several advantages; for example, high time resolution is not necessary for the temperature measurement, and a large S/N ratio can be obtained by long exposure time and averaging. Also, compared with the method by Gallagher and Fenn [7], utilization of emission spectroscopy simplifies the measurement, and measuring plasma temperatures by emission spectroscopy is advantageous because it is nonintrusive to the plasma. Based on several assumptions (see Sec. III), Z_r can be calculated from the axial distributions of the T_t and T_r directly measured by emission spectroscopy.

The emission spectroscopic method to determine T_t and T_r of hydrogen plasma was developed in our previous studies [16,17]. The T_t of atomic hydrogen was determined by spectral profile fitting of the Balmer H_β line [16], and T_r of molecular hydrogen was determined by spectral line intensity fitting of the Fulcher- α band of molecular hydrogen [17].

The objective of this current work was to develop a method that can experimentally determine Z_r of molecular hydrogen by using a steady nonequilibrium plasma jet and emission spectroscopy. In this method, first, a steady nonequilibrium plasma jet was produced using experimental apparatus. Then, T_t and T_r were measured using emission spectroscopy. Finally, Z_r of molecular hydrogen was obtained based on these experimental data. The outline of this paper is as follows. Section II describes the experimental apparatus and the temperature measurement methods. Section III first describes the experimental results, then describes how Z_r is determined from these experimental results, and finally compares the obtained Z_r with that in the literature. Section IV summarizes the conclusions of this study.

II. Experimental Setup

Figure 2 shows the experimental apparatus used to produce a steady nonequilibrium plasma jet. Hydrogen was used as a test gas. The plasma was produced by using inductive heating at low pressure. The induced electric current, which was caused by temporal variation in the radio-frequency (RF) magnetic field, accelerated the electrons

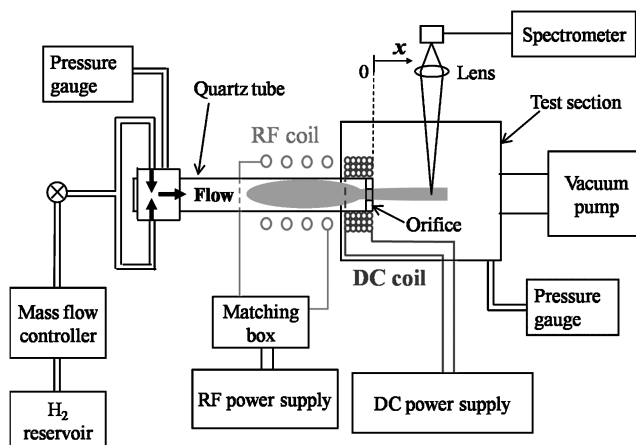


Fig. 2 Experimental apparatus.

that collided with neutral particles and caused chemical reactions such as dissociation and ionization. As a result, a weakly ionized plasma consisting of H_2 , H , H^+ , and e^- was produced. A quartz tube with an inner/outer diameter of 46/50 mm was surrounded by four turns of a water-cooled RF coil. An RF power supply operating at a frequency of 13.56 MHz and maximum output power of 2 kW was connected to a matching network that cancels the power reflected from the plasma. The test gas was regulated using a mass flow controller and was injected through two opposing ports. Downstream of the RF coil was a direct current (DC) coil connected to a DC power supply that had a maximum current of 256 A. This DC coil was made by wrapping 3-mm diameter copper tubing around the quartz tube. The copper tubing was cooled by water flowing through the tubing, and each turn was insulated by thermal shrinking tube. This DC coil generated a DC convergent-divergent magnetic field that squeezed and compressed the plasma flow to the center line, thus decreasing the heat loss on the wall of the quartz tube [18]. An orifice plate (orifice diameter of 6 mm and plate thickness of 5 mm) was installed at the downstream end of the quartz tube. At this orifice, the plasma flow was exhausted as a sonic jet, and accelerated to supersonic speed by expansion in the test section. The combination of the DC magnetic field and the orifice plate converted the plasma source generated by the RF coil into a supersonic plasma jet. Figure 3 shows a photo of the generated supersonic hydrogen plasma jet. The coordinate system is also shown in Fig. 3, where position $x = 0$ mm is just at the orifice exit. Table 1 summarizes the experimental condition. The total pressure of the exiting jet was measured at the static port on the orifice plate, because the flow in front of the orifice is quite slow and thus the reservoir condition was expected to hold there. The total pressure is 211 ± 18 Pa. The Knudsen number calculated for the orifice diameter was 0.05, thus indicating that the plasma flow used in this study could be categorized as slip flow [19].

Both T_t and T_r were determined using emission spectroscopy. The T_t of the atomic hydrogen was determined by spectral profile fitting of the Balmer H_β line [16]. Based on the estimation of the factors contributing to H_β line broadening, T_t in the present plasma was determined by H_β line profile fitting, taking into account

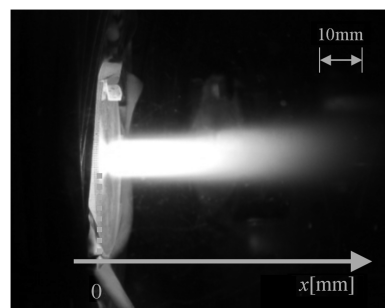


Fig. 3 Hydrogen plasma jet produced by the apparatus.

Table 1 Experimental condition

Mass flow rate, H ₂	8.4 × 10 ⁻⁷	kg/s
Input RF power	1.0	kW
DC coil current	50	A
DC magnetic field flux at the center of DC coil	42	mT
Average specific enthalpy	360	MJ/kg
Total pressure	211	Pa
Ambient pressure in test section	20	Pa
Knudsen number for orifice diameter	0.05	

Table 2 Gratings used to measure translational and rotational temperatures

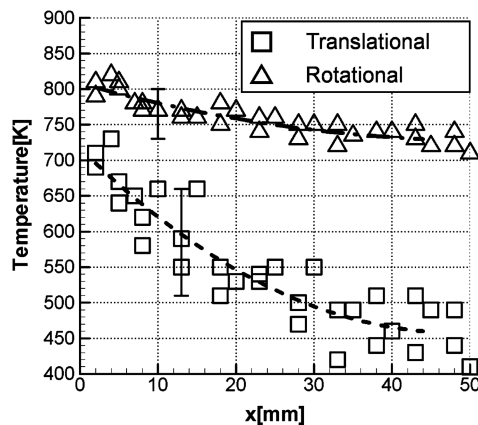
Measured temperature		T_t	T_r
Number of grooves	gr/mm	3600	600
Measurement resolution	nm	0.00780	0.080
Wavelength width observed for a single data sampling	nm	7.98	82
Exposure time	ms	20–1000	200–2000

instrumental broadening, Doppler broadening, and spin-orbit coupling. The T_r of molecular hydrogen was determined by spectral line intensity fitting of the Fulcher- α band of molecular hydrogen [17]. This fitting method simultaneously determines T_r , T_v , and T_e . Assuming the presence of a unique T_t for the gas mixture, we experimentally investigated the translational-rotational relaxation of molecular hydrogen. Figure 2 also shows the optical system in the emission spectroscopic method. The measurement point was determined by the lens system installed in front of the spectrometer. The emission focused by the lens was directed into the spectrometer (Hamamatsu, PMA-50) through an optical fiber. The spot size of the detected emission at the measurement point was 2 mm. Two gratings were used, one for T_t and the other for T_r (Table 2). The exposure time for a single sample depended on the emission intensity at the measurement point. During all measurements, temporal variation in the emission intensity was within $\pm 3\%$, indicating steady plasma flow. The measured data were obtained by averaging 4–10 samples. An Abel inversion was not done in this work, because the radial uniformity in the emission region was already confirmed in past works by the authors [17,18].

III. Results and Discussion

A. Experimental Results

The axial distributions of T_t and T_r are shown in Fig. 4, where $x = 0$ mm is at the orifice exit and $x = 2$ mm is at the most upstream measurement point. No optical measurements were done at $x < 2$ mm because the spot size of our optical system was 2 mm. The

**Fig. 4** Axial distributions of translational and rotational temperatures.

error bars for T_t and T_r indicate variations in the 5 experiments, and confirm good repeatability in the measurements. Emission spectroscopy near the RF coil region (upstream of the orifice) revealed that T_t and T_r were in equilibrium and were around 1900 K. However, due to the strong free expansion at the orifice exit, T_t rapidly decreased at $x > 0$, and the translational energy was converted into the flow kinetic energy. In contrast, the decrease in T_r was gradual due to the slow translational-rotational relaxation. The axial distributions of T_v and T_e are shown in Fig. 5, indicating that both the vibrational mode of molecular hydrogen and the electron translational mode were frozen.

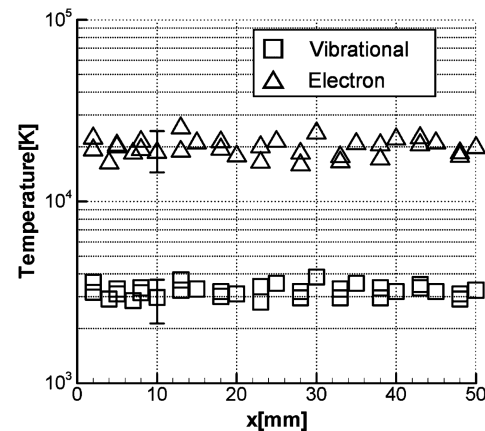
B. Model to Determine Rotational Relaxation Collision Number

A model was developed to determine Z_r from the axial distributions of T_t and T_r shown in Fig. 4, which were directly measured using emission spectroscopy. This model has the following assumptions: 1) T_t and T_r are equal upstream of the orifice, 2) vibrational and electronic excitation modes of molecular hydrogen are frozen from upstream to downstream, 3) the gas component is only molecular hydrogen, and the effect of the other chemical species is negligible, 4) Mach number is 1 at $x = 0$ mm, and 5) both T_t and T_r at $x = 0$ mm are equal to T_r at $x = 2$ mm.

Assumptions 1 and 2 are based on the experimental results. Although the electronic excitation temperature of molecular hydrogen was not measured, the assumption of a frozen electronic excitation mode is considered reasonable taking the frozen vibrational and electron translational modes into account. Assumption 3 is based on previous experimental results [16]; in the plasma flow generated by the present experimental apparatus, the degree of dissociation was less than 10% [16], and the major species is molecular hydrogen. Assumption 4 is based on the aerodynamics. Although Mach number can be calculated using the specific heat ratio γ and T_t , the value of γ is not clear in the nonequilibrium and relaxed flow. The value of γ here is treated as an uncertainty, and accurate determination of γ is not discussed in this work. The discussion on γ is described in Sec. III.C. Assumption 5 can be explained as follows: because of the strong free expansion, T_t decreases immediately after the flow is exhausted at $x = 0$, and therefore $T_t(x = 0) > T_t(x = 2)$. However, because the rotational mode is frozen just downstream of the exit, $T_r(x = 0) = T_r(x = 2)$. Assuming the translational and rotational modes are in equilibrium inside the orifice, $T_t(x = 0) = T_r(x = 0)$. Therefore, $T_t(x = 0) = T_r(x = 0) = T_r(x = 2)$. Assumption 5 enables calculation of the equilibrium temperature between translational and rotational modes by using the experimental data for T_t and T_r at $x = 2$ mm.

Assuming one-dimensional flow based on radial uniformity, translational-rotational relaxation equation can be expressed as follows [7]:

$$u \frac{dT_r}{dx} = \frac{T_t - T_r}{\tau_r} \quad (1)$$

**Fig. 5** Axial distributions of vibrational and electron temperatures.

In this analytical model, we assume that the plasma flow consists only of molecular hydrogen. Thus, τ_r is given by

$$\tau_r = Z_r \tau_c = Z_r \frac{\lambda}{v_{th}} = Z_r \frac{1}{\sqrt{2} \pi d^2 n} \sqrt{\frac{\pi m}{8 k T_t}} = \frac{Z_r}{4 d^2 n} \sqrt{\frac{m}{\pi k T_t}} \quad (2)$$

Substituting Eq. (2) into Eq. (1) yields Z_r as follows:

$$Z_r = \frac{4 d^2 n}{u} \sqrt{\frac{\pi k T_t}{m}} \left(\frac{dT_r}{dx} \right)^{-1} (T_t - T_r) \quad (3)$$

In Eq. (3), T_t , T_r , and dT_r/dx are obtained as experimental data. The variables d , u , and n are calculated using these experimental data as follows: d is calculated as a function of T_t based on the variable hard sphere (VHS) model [20]:

$$d = d_{ref} \left(\frac{T_t}{T_{ref}} \right)^{\frac{1-2\omega}{4}} \quad (4)$$

where d_{ref} , T_{ref} , and ω were set to 2.42×10^{-10} m, 1000 K, and 0.84, respectively, which were determined by fitting the momentum transfer cross section of H_2 - H_2 collision [20–22] as shown in Fig. 6.

The variable u was calculated using the energy balance as follows:

$$\frac{1}{2} u^2 + \frac{5}{2} R T_t + R T_r = \frac{7}{2} R T_s (\text{const}) \quad (5)$$

$$\therefore u = \sqrt{R(7T_s - 5T_t - 2T_r)} \quad (6)$$

where T_s can be calculated using the T_t and T_r measured at $x = 2$ mm, based on the assumptions 4 and 5. Because the vibrational and electronic excitation modes are considered to be frozen from the upstream to the downstream of the orifice, Eq. (5) does not include the contribution of these modes.

n is calculated assuming isentropic relation as follows:

$$n = n_0 \frac{n}{n_0} = \frac{p_0}{k T_s} \left(\frac{T_t}{T_s} \right)^{\frac{1}{\gamma-1}} \quad (7)$$

The relative error in Z_r can be calculated based on the errors in p_0 , T_t , and T_r :

$$\frac{\Delta Z_r}{Z_r} = \sqrt{\left(\frac{\partial Z_r}{\partial p_0} \frac{\Delta p_0}{Z_r} \right)^2 + \left(\frac{\partial Z_r}{\partial T_t} \frac{\Delta T_t}{Z_r} \right)^2 + \left(\frac{\partial Z_r}{\partial T_r} \frac{\Delta T_r}{Z_r} \right)^2} \quad (8)$$

where

$$\frac{\partial Z_r}{\partial p_0} \frac{\Delta p_0}{Z_r} = \frac{\Delta p_0}{p_0} \quad (9)$$

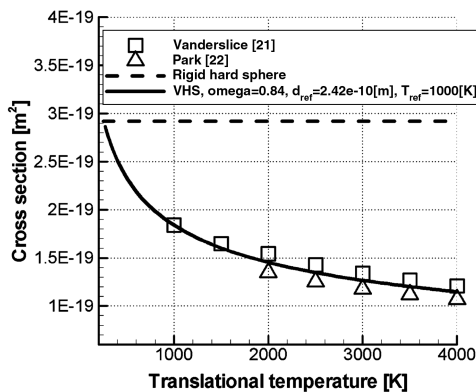


Fig. 6 Momentum transfer cross section of H_2 - H_2 collision.

$$\frac{\partial Z_r}{\partial T_t} \frac{\Delta T_t}{Z_r} = \left[\frac{1}{T_t - T_r} \left\{ \frac{2\gamma - 1}{\gamma - 1} - \omega - \left(\frac{\gamma + 1}{\gamma - 1} - \omega \right) \frac{T_r}{T_t} \right\} + \frac{5}{2(7T_s - 5T_t - 2T_r)} \right] \Delta T_t \quad (10)$$

$$\frac{\partial Z_r}{\partial T_r} \frac{\Delta T_r}{Z_r} = \left[-\frac{1}{T_t - T_r} + \frac{1}{7T_s - 5T_t - 2T_r} \right] \Delta T_r \quad (11)$$

C. Obtained Rotational Relaxation Collision Number

The axial distributions of T_t and T_r are shown in Fig. 4. Because of the scatter in the experimental data, we fitted the data by using the least-square method. Then, Z_r was determined using these data and the procedure described in Sec. III.B.

Figure 7 shows that for $500 < T_r < 700$ K, the obtained Z_r ranged from 70 to 150. In Eqs. (5) and (6), T_s ranged from 920–930 K, and the corresponding enthalpy, except the vibrational and electronic excitation modes, was 9.6 MJ/kg. This value of T_s is much smaller than the translational and rotational temperatures in RF coil region (1900 K, see Sec. III.A). This is probably due to the heat loss on the quartz tube and the orifice. The Mach number at $x = 30$ mm was 2.0 for $\gamma = 1.4$. The two curves for the obtained Z_r in Fig. 7 were drawn considering the uncertainties in T_t , T_r , p_0 , and γ . Equations (8–11) were used to estimate the uncertainties in T_t , T_r , and p_0 . Because the meaning of γ in assumption 4 and in the isentropic relation of Eq. (7) is ambiguous, and thus the most appropriate value of γ is not clear, two cases were considered in estimating the uncertainty in γ , namely, with and without contribution from the specific heat of vibrational mode as follows:

$$\gamma_1 = \frac{2.5R + R + C_{v,vib}}{1.5R + R + C_{v,vib}}, \quad C_{v,vib} = R \left(\frac{\theta_v}{T_v} \right)^2 \frac{\exp(\frac{\theta_v}{T_v})}{[\exp(\frac{\theta_v}{T_v}) - 1]^2},$$

and

$$\gamma_2 = 1.4$$

The obtained Z_r was larger when γ_2 was used compared with that when γ_1 was used. The respective contribution of the uncertainties in T_t , T_r , p_0 , and γ on the error in the calculated Z_r is 13, 23, 8, and 56% on average.

Figure 7 also shows the Z_r values reported in previous studies. The value of Z_r obtained in this work agrees well with some of those previously values, which were reported in the 1960s–70s [1,2,5–8]. Furthermore, Z_r obtained in this work supports the theoretical results by Sharma [3] in 1994 and those by Furudate et al. [4] in 2006, which are two of the latest results obtained using the master equations. Although our experimental results are not sufficiently decisive to determine Z_r of molecular hydrogen and the temperature range of the

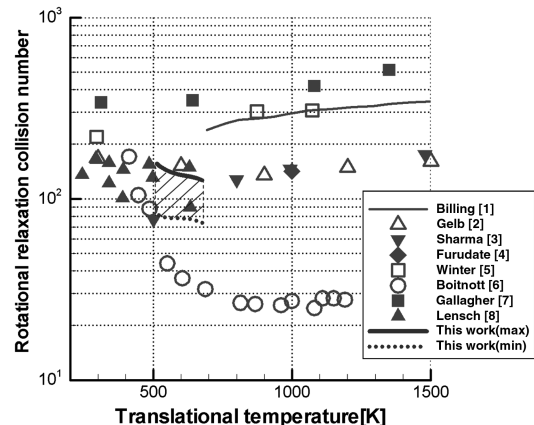


Fig. 7 Comparison of rotational relaxation collision number obtained in this work with that in the literatures.

obtained Z_r was limited, the method to determine Z_r by using a steady plasma jet and emission spectroscopy was successfully demonstrated. The basic idea of the present method can be applied to other relaxation processes and other chemical species, if the method to determine the necessary temperatures by emission spectroscopy is established, and their relaxation is observed in the experiments.

In the future, increasing the input power for the plasma generation and installing a cooling system for the glass tube will enable experimental determination of Z_r for a wider temperature range. Moreover, the temperature distributions will be numerically calculated by direct simulation Monte Carlo method using Z_r obtained in the experiments. The comparison of the temperature distributions will evaluate the experimental results.

Another future improvement will be to increase the operating pressure, which will enable observation of the translational-vibrational relaxation because the translational-vibrational relaxation time will then be longer than the translational-rotational relaxation time.

IV. Conclusions

A method to experimentally determine the relaxation collision number by using a steady plasma jet and emission spectroscopy was developed. The advantages of this method are that 1) the direct measurement of the temperatures is possible by emission spectroscopy, 2) the measurement is simple and easy, 3) the measurement is nonintrusive to the flow, and 4) a large S/N ratio can be obtained by the steadiness of the jet. The method was validated by using it to determine the rotational relaxation collision number of molecular hydrogen as follows. First, a translational-rotational nonequilibrium hydrogen plasma jet was generated by strong free expansion at an orifice exit, and relaxation of the molecular hydrogen was successfully observed downstream by emission spectroscopy. Then, the translational temperature was determined by fitting the Balmer H_β line profile, and the rotational temperature was determined by line-intensity fitting of the Fulcher- α band. Finally, incorporating several assumptions based on this experimental data, the rotational relaxation collision number of molecular hydrogen was determined as 70–150 for the temperature range of 500–700 K. These results support two of the latest theoretical studies.

Acknowledgments

This work was supported by Grant-in-Aid for Scientific Research Nos. 18.11672, 17360408, and 21360413 of the Japan Society for the Promotion of Science. The primary author was supported by research fellowships of the Japan Society for the Promotion of Science for Young Scientists.

References

- [1] Billing, G. D., "Rotational and Vibrational Relaxation of Hydrogen and Deuterium," *Chemical Physics*, Vol. 20, No. 1, 1977, pp. 35–42. doi:10.1016/0301-0104(77)85111-2
- [2] Gelb, A., and Alper, J. S., "Classical Trajectory Study of Rotational Relaxation Times of Molecular Hydrogen," *Chemical Physics Letters*, Vol. 31, No. 2, 1975, pp. 245–247. doi:10.1016/0009-2614(75)85012-3
- [3] Sharma, S. P., "Rotational Relaxation of Molecular Hydrogen at moderate Temperatures," *Journal of Thermophysics and Heat Transfer*, Vol. 8, No. 1, 1994, pp. 35–39. doi:10.2514/3.498
- [4] Furudate, M., Fujita, K., and Abe, T., "Coupled Rotational-Vibrational Relaxation of Molecular Hydrogen at High Temperatures," *Journal of Thermophysics and Heat Transfer*, Vol. 20, No. 3, 2006, pp. 457–464. doi:10.2514/1.16323
- [5] Winter, T. G., and Hill, G. L., "High-Temperature Ultrasonic Measurements of Rotational Relaxation in Hydrogen, Deuterium, Nitrogen, and Oxygen," *Journal of the Acoustical Society of America*, Vol. 42, No. 4, 1967, pp. 848–858. doi:10.1121/1.1910657
- [6] Boinnott, C. A., and Warder, R. C. Jr., "Shock-Tube Measurements of Rotational Relaxation in Hydrogen," *Physics of Fluids*, Vol. 14, No. 11, 1971, pp. 2312–2316. doi:10.1063/1.1693335
- [7] Gallagher, R. J. J., and Fenn, J. B., "Rotational Relaxation of Molecular Hydrogen," *Journal of Chemical Physics*, Vol. 60, No. 9, 1974, pp. 3492–3499. doi:10.1063/1.1681565
- [8] Lensch, G., and Gronig, H., "Experimental Determination of Rotational Relaxation in Molecular Hydrogen and Deuterium," *Proceedings of the Eleventh International Symposium on Shock Tubes and Waves*, Univ. of Washington Press, Seattle, WA, 1977, pp. 132–139.
- [9] Parker, J. G., "Rotational and Vibrational Relaxation in Diatomic Gases," *Physics of Fluids*, Vol. 2, No. 4, 1959, pp. 449–462. doi:10.1063/1.1724417
- [10] Lordi, J. A., and Mates, R. E., "Rotational Relaxation in Nonpolar Diatomic Gases," *Physics of Fluids*, Vol. 13, No. 2, 1970, pp. 291–308. doi:10.1063/1.1692920
- [11] Greenspan, M., "Rotational Relaxation in Nitrogen, Oxygen, and Air," *Journal of the Acoustical Society of America*, Vol. 31, No. 2, 1959, pp. 155–160. doi:10.1121/1.1907686
- [12] Boyd, I. D., "Monte Carlo Simulation of Nonequilibrium Flow in a Low-Power Hydrogen Arcjet," *Physics of Fluids*, Vol. 9, No. 10, 1997, pp. 3086–3095. doi:10.1063/1.869474
- [13] Boyd, I. D., Beattie, D. R., and Cappelli, M. A., "Numerical and Experimental Investigations of Low-Density Supersonic Jets of Hydrogen," *Journal of Fluid Mechanics*, Vol. 280, No. -1, 1994, pp. 41–67. doi:10.1017/S0022112094002843
- [14] Rabitz, H., and Lam, S.-H., "Rotational energy relaxation in molecular hydrogen," *The Journal of Chemical Physics*, Vol. 63, No. 8, 1975, pp. 3532–3542. doi:10.1063/1.431792
- [15] Miller, D. R., and Andres, R. P., "Rotational Relaxation of Molecular Nitrogen," *The Journal of Chemical Physics*, Vol. 46, No. 9, 1967, pp. 3418–3423. doi:10.1063/1.1841233
- [16] Takama, Y., and Suzuki, K., "Spectroscopic Observation of Translational-Rotational Nonequilibrium in Low-Density Hydrogen Plasma Flow," *Journal of Thermophysics and Heat Transfer*, Vol. 23, No. 3, 2009, pp. 454–462.
- [17] Takama, Y., and Suzuki, K., "Spectroscopic Diagnostics of Thermochemical Nonequilibrium Hydrogen Plasma Flow," *Journal of Thermophysics and Heat Transfer*, Vol. 21, No. 3, 2007, pp. 630–637. doi:10.2514/1.28288
- [18] Takama, Y., and Suzuki, K., "Experimental Studies on Nonequilibrium Plasma Flow in a Convergent-Divergent Magnetic Field," *Plasma Sources Science and Technology*, Vol. 17, No. 1, 2008, p. 015005. doi:10.1088/0963-0252/17/1/015005
- [19] Tsien, H. S., "Superaerodynamics, Mechanics of Rarefied Gases," *Journal of the Aeronautical Sciences*, Vol. 13, No. 12, 1946, pp. 653–664.
- [20] Bird, G. A., *Molecular Gas Dynamics and the Direct Simulation of Gas Flows*, Clarendon Press, Oxford, 1994, pp. 68, 409.
- [21] Vandersllice, J. T., Weissman, S., Manson, E. A., and Fallon, R. J., "High-Temperature Transport Properties of Dissociating Hydrogen," *Physics of Fluids*, Vol. 5, No. 2, 1962, pp. 155–164. doi:10.1063/1.1706590
- [22] Park, C., "Chemical-Kinetic Parameters of Hyperbolic Earth Entry," *Journal of Thermophysics and Heat Transfer*, Vol. 15, No. 1, 2001, pp. 76–90. doi:10.2514/2.6582